A NOVEL DEEP LEARNING MODEL FOR BREAST CANCER CLASSIFICATION USING HISTOPATHOLOGY IMAGES

Article *in* Jilin Daxue Xuebao (Gongxueban)/Journal of Jilin University (Engineering and Technology Edition) · March 2023

DOI: 10.17605/OSF.IO/WNQ34

6 authors, including:

Arslan Akram
Superior University
12 PUBLICATIONS **18** CITATIONS
SEE PROFILE

Asad Razzaq
University of Toyama
5 PUBLICATIONS **17** CITATIONS
SEE PROFILE

Sobia Yaqoob
Government College University Faisalabad
9 PUBLICATIONS **60** CITATIONS
SEE PROFILE

Jilin Daxue Xuebao (Gongxueban)/Journal of Jilin University (Engineering and Technology Edition)
ISSN：1671-5497
E-Publication: Online Open Access
Vol: 42 Issue: 03-2023
DOI 10.17605/OSF.IO/WNQ34

A NOVEL DEEP LEARNING MODEL FOR BREAST CANCER CLASSIFICATION USING HISTOPATHOLOGY IMAGES

BARZA ATTIQUE KHARI
MS Scholar, Department of Computer Science, University of Okara, Okara, Pakistan.
Email: barzaattiquekhari@gmail.com

ARSLAN AKRAM
SSE CS, Department of School Education (PSED) Okara, Okara, Pakistan.
Phd Scholar, Department of Computer Science, Superior University Lahore, Lahore, Pakistan.
Email: aaadoula11@gmail.com

NAHEED AKHTAR
Lecturer, Department of Computer Science, University of Education Lahore, Lahore, Pakistan.
Email: naheedswl@ue.edu.pk

RAZZAQ ASAD
PhD Scholar, Graduate School of Science and Engineering, University of Toyama, Toyama, Japan.
Email: asad9731@gmail.com

SOBIA YAQOOB*
Lecturer, Department of Computer Science, University of Okara, Okara, Pakistan.
PhD Scholar, Department of Computer Science, Superior University Lahore, Lahore, Pakistan.
*Corresponding Author Email: sobia.yaqoob@uo.edu.pk

Dr. FAHAD SARDAR
MBBS, FCPS, Xian Medical University China, China. Email: drfahds@gmail.com

Abstract

Early metastasis detection is a crucial prognostic factor for breast cancer patients. The current clinical process is a laborious and manual workload on pathologists. These factors have driven recent research in applying deep learning techniques towards breast cancer detection. The resulting state-of-the-art systems can perform comparably to pathologists for tumour detection within pathology slides. However, these systems are not clinically viable as they require significant time or compute power to process high-resolution images. This project's objective was to investigate breast cancer detection via deep learning techniques using low-resolution whole-slide images. The intent was to reveal whether machine learning models could be developed that provide high confidence results using fractional resources by using low- versus high-resolution images. A deep learning pipeline has been developed which reduces high-resolution whole-slide images to a sufficiently small size so they can be fed as input into a CNN for binary classification (i.e., cancer or normal). Several improvements have been implemented to boost general performance, namely supplementing the training data, adding data augmentations, and applying tissue detection. Ultimately, the developed low-resolution models are effectively skill-less for very low-resolution inputs. An observed significant decrease in model inference time is a superficial benefit given the loss in classification capability. This is a promising and expected result arising from an obvious limitation with the methodology; very low resolutions, effectively zooming out on a slide, preserves only information about macro-cellular structures which is often insufficient alone to detect cancer. In conclusion, the developed deep learning pipeline is suitable as a clinically viable cancer detection system when using the input resolutions investigated. Thus, this deep learning pipeline is insufficient as a prior filter to quickly classify easy pathology cases, which would justify use of the slow, high-performance BreakHis submissions for difficult but rare cases. There may exist some optimal input resolution that balances prediction performance and resource requirements which was not empirically investigated in this project.

Jilin Daxue Xuebao (Gongxueban)/Journal of Jilin University (Engineering and Technology Edition)
ISSN：1671-5497
E-Publication: Online Open Access
Vol: 42 Issue: 03-2023
DOI 10.17605/OSF.IO/WNQ34

Keywords: Deep Learning; Convolutional Neural Networks; Medical Image Analysis; Breast Cancer Detection; Whole-Slide Classification; Whole-Slide Images; Low Resolution; Kaggle; BreakHis

1. INTRODUCTION

One of the most serious public health issues is breast cancer. Along with heart attacks, it is a common cause of death. In women, it is predicted that about 30% of all newly diagnosed malignancies will be breast cancer by 2022. In the United States, women are predicted to be diagnosed with 287,850 new instances of invasive breast cancer whereas 51,400 new cases of non-invasive breast cancer are predicted this year. In the United States, breast cancer is estimated to kill 43,250 people this year. Moreover, statistics tells that approximately 3.8 million women had breast cancer as of January 2022. Research tells that around 1 in 833 men may suffer from this disease. Invasive breast cancer in men is expected to increase by 2,710 new cases in the United States by 2022. [1].

Mutations or aberrant alterations in the genes that govern cell development and health are the causes of cancer. It might develop into a malignant/cancerous or benign/non-cancerous breast cyst. Histopathology is a discipline of pathology that entails taking a small sample of tissue from a contaminated breast and examining it under a microscope. There are many approaches to diagnosing cancer, including magnetic resonance imaging and fine-needle aspiration cytology. However, histopathology is a standardized procedure for the diagnosis of breast cancer and guarantees its result accuracy when compared to other cancer diagnostic approaches. Investigation through histopathology is a complex and time-consuming road to cancer diagnostic information. However, the strong professional experience of pathologists is crucial for the physical diagnosis of breast cancer which is time consuming, costly and misdiagnosis may also occur [2].

By introducing a faster and more accurate diagnostic approach, CAD “computer-assisted diagnostic” may help to reduce the use of specialists. CAD models working with “Machine learning algorithms” have shown favorable results in examining breast tissues using histology. Authentic dataset or medical records in form of textual or image data is fed into CAD models to get trained. Data is said to be imbalanced if one sample type has a higher no. of instances than the other. In the case of unfair distribution of data records, classification results are weighted toward the class having more instances which leads to misdiagnosis.

Classification and prediction are done through several algo rithms available e.g., J48, K-NN, and Naive Bayes, which are several existing classifiers in machine learning. The classification results of breast cancer disorders are produced using a support vector machine "SVM" technique in this study. The most typical measures used to assess the model's performance are accuracy, precision, and sensitivity [3]–[7].

This study presents an ML-based method for classifying the breast cancer images as malignant and benign. A curvelet transformation is used to extract features of interest. Then the support vector machine is utilized to save time and enhance overall precision. This research work provides a low-cost high-precision solution for a variety of time modalities. The proposed strategy has successfully produced positive comparable results.

Jilin Daxue Xuebao (Gongxueban)/Journal of Jilin University (Engineering and Technology Edition)
ISSN：1671-5497
E-Publication: Online Open Access
Vol: 42 Issue: 03-2023
DOI 10.17605/OSF.IO/WNQ34

One of the distinguishing features of this study is that it covers a broad range of disease informational records. The generalizability of the study is demonstrated by the results obtained for three data sets with distinct features. To put it another way, the proposed method is not dependent on the data set. Therefore, a different set of data can also be passed to the model with comparable accuracy.

Traditional learning procedures can provide as many successful results as deep learning methods, according to this study. Attempt to make a decision-support system that can assist medical professionals in making decisions by allowing accurate detection of breast cancer malignancy using Machine Learning and image processing methods.

The following are the four sections of this work. Section 2 relates the associated existing work while Section 3 contains the highlights of the dataset used in this evaluation and recommended framework. Section 4 presents and analyses the findings of the evaluation, and comparisons with previous studies. The final section 5 summarizes the work and provides guidelines for future research.

2. LITERATURE REVIEW

Researchers have proposed numerous strategies for BC diagnosis in histopathology images in the last few years. The medical context regarding breast cancer diagnosis in pathology slides is established. The historiography of breast cancer detection is surveyed, from manual conventional diagnosis to automated state-of-the-art deep learning techniques. Current state-of-the-art techniques are surveyed in depth by assessing submissions of different ML and DL techniques using different histopathology datasets. Other techniques using low-resolution images from the broader field of medical image analysis are also considered. Thus, this chapter places this project within the medical image analysis context and provides guidance for design decisions pertaining to this project's developed low-resolution image models.

The severity of a patient's cancer diagnosis is dependent on the stage of the cancer. Cancer staging is determined by factors such as the size and location of the tumor, and more importantly whether the cancer has metastasized (i.e., the cancer has spread). Prognosis for breast cancer patients in England is generally optimistic, with an average 5-year overall survival rate of 85%. However, this significantly deteriorates to 26.2% when the breast cancer metastasizes .The early diagnosis of breast cancer can improve prognosis and chance of survival, crucially so when the presence of metastases is established. Even when metastases are not present, the accurate classification of such can prevent patients undergoing unnecessary, possibly detrimental treatments.

Breast cancer is likely to form in the ducts and lobes, with nearby axillary lymph nodes (small glands that filter lymph fluid through the lymphatic system) in the underarm being the first-place breast cancer is likely to spread [8]. Thus, metastatic involvement of lymph nodes is one of the most important prognostic variables in breast cancer. It is also an important predictive factor for the presence of distant metastases as the lymphatic system distributes across the human body.

Jilin Daxue Xuebao (Gongxueban)/Journal of Jilin University (Engineering and Technology Edition)
ISSN：1671-5497
E-Publication: Online Open Access
Vol: 42 Issue: 03-2023
DOI 10.17605/OSF.IO/WNQ34

L. J. Martin (2020) outlines the tissue extraction process needed for pathological analysis. Patients undergo sentinel node biopsy, a method that ensures only lymph nodes most likely to have cancer are removed. This minimizes the invasiveness of lymph node extraction. A tracer (e.g., radioactive substance or dye) is injected into the area around a tumor to identify the lymph nodes the tumor drains into, which are referred to as sentinel lymph nodes. One to three sentinel nodes are usually removed to be tested for cancer. Then, fixation is carried out on the extracted sentinel nodes; the nodes are processed to make glass slides that hold tissue sections just a few micrometers thick (3 to 5 slides per lymph node) [9]. Typically, stains are added to the glass slides to make the tissue cells more visible (the cells would otherwise be transparent) [10]. Stains usually employ immuno-histochemistry to highlight the presence of proteins normally found in breast cancer cells and not in lymph nodes, which aims to improve pathologist sensitivity. However, immuno-histochemistry testing of sentinel lymph nodes increases cost and slide preparation time. Even with immuno-histochemistry stained slides, the identification of small cancer metastases can be tedious and inaccurate. The hematoxylin and eosin (H&E) stain is most widely used across many different tissue types, inducing sharp blue and pink contrasts across various (sub)cellular structures [10].

Conventionally, the diagnostic procedure involves the glass slides being inspected by a pathologist (a doctor who diagnoses and studies disease involving cells and tissue samples) under a microscope to determine whether metastases are present. The task consists of the localization and identification of small lesions in the full slide space. There are three distinct categories of breast cancer lesion a pathologist seeks to identify (see Table 2.1): isolated tumor cells (ITCs), micro-metastases, and macro-metastases.

In conventional breast cancer diagnosis, diagnostic accuracy is dependent on a pathologist’s experience, which is built up over many years of observations of different patient tissue samples and confirmed diagnoses [11]. However, high diagnostic accuracy cannot be guaranteed. The most senior of pathologists can miss metastases, especially in the case of micro-metastases and isolated tumor cells, which are difficult to detect given the large area of tissue that has to be examined per slide [12]. Even if pathologists were perfectly accurate, the task is time consuming and labor intensive, requiring large amounts of reading time through extensive microscope assessment [13]. For example, in the Camelyon-16 challenge, a pathologist without time constraints required roughly 30 hours to exhaustively analyze 129 slides and missed 27.6% of metastases. Furthermore, the imposition of time constraints to simulate clinical requirements resulted in a panel of 11 pathologists missing a mean of 37.2% of metastases (median 120 minutes to analyze the same 129 slides). In the majority of cases, pathologists are investigating benign tissue (i.e., absence of metastases); 60{70% of sentinel lymph nodes do not contain any metastases. Thus, a disadvantageous proportion of a pathologist’s workload is spent simply confirming negative cases. When metastases are identified, the tissue samples are prone to misinterpretation and may require repeat assessments involving multiple pathologists. A retrospective study showed that review of slide diagnoses by pathology experts changed the nodal status in 24% of patients [14].

Jilin Daxue Xuebao (Gongxueban)/Journal of Jilin University (Engineering and Technology Edition)
ISSN：1671-5497
E-Publication: Online Open Access
Vol: 42 Issue: 03-2023
DOI 10.17605/OSF.IO/WNQ34

Automated breast cancer detection using histopathology slides is a research area within the more general field of digital pathology - the study of disease in tissue specimens using virtual microscopy. Pathology slides have been digitized since before whole-slide imaging scanners became commercially available in the 1990s. Pathologists could create partial-slide images containing regions of interest [15]. Computer-aided diagnosis emerged as a result, where digital tools are utilized to aid the diagnostic procedure. However, cancer detection was still a completely manual task carried out by pathologists. In fact, computer-aided diagnosis was rarely adopted into the regular workflows of pathologists due to issues with the digital nature of the slide images, such as color variations in monitors unnecessarily complicating assessments [16].

The emergence of digital pathology facilitated new medical procedures, such as telepathology in the 1980s. In telepathology, digital slide images are communicated between labs for remote pathology diagnosis. Several advantages arise from this practice: low resource labs can employ the expertise of top (international) academic centers, second opinions can be more easily requested via remote consults, and physical shipping/storage of fragile glass slides is mitigated Telepathology is especially beneficial where remote diagnosis is essential, such as with intra-operative frozen section procedures. Intra-operative frozen section procedures are used for rapidly preparing histo-Pathology slides for inspection during surgery. In breast cancer diagnosis, this assists in determining whether further lymph nodes need to be extracted - a crucial decision in breast conserving surgery (i.e., lumpectomy or partial mastectomy) [17]. Diagnosis in such procedures is manually conducted by a remote pathologist; thus, digital pathology should be distinguished from automated pathology.

As computational power and medical data became more available for research, machine learning techniques were applied for automated cancer detection. These techniques typically involved human engineers collaborating with pathologists to determine hand-crafted features about the problem domain (e.g., mitoses, uniformity of cell size, and uniformity of cell shape). The features are manually decided, but their association to the predictions is learnt automatically. This marked a shift in breast cancer diagnosis from manual human-based diagnostic systems to automated systems that are trained by computers using human-driven hand-crafted features. Such systems could mitigate subjectivity and variability in pathology diagnosis. The use of hand-crafted features tends to provide prediction transparency and, hence, are intuitive to a pathologist or clinician. This is vital for diagnosis as decision accountability is required. However, deriving such hand-crafted features is challenging since this involves a fundamental understanding of the nature of the disease and its manifestation within tissue [1].This issue drives research in deep learning techniques, which involve automatic feature discovery .

Machine learning techniques mainly perform classification or regression [18]. Fundamentally, classification involves predicting some label, whilst regression involves predicting some quantity. Classification is more pertinent to automated breast cancer diagnosis; metastasis detection requires qualifying, not quantifying. Classification can be further separated into two forms that concern this project: whole-slide classification and tumor localization. Whole-slide classification involves the slide-level prediction of

Jilin Daxue Xuebao (Gongxueban)/Journal of Jilin University (Engineering and Technology Edition)
ISSN：1671-5497
E-Publication: Online Open Access
Vol: 42 Issue: 03-2023
DOI 10.17605/OSF.IO/WNQ34

metastasis, either with binary labels (i.e., metastasis or normal), or with multi-class labels (i.e., no cancer, isolated tumor cells, micro-metastases, or macro-metastases). Tumor localization refers to identifying and segmenting metastases within a slide. This typically involves pixel-wise or patch-based classification, where the status of every pixel (or groups of pixels) in an image is predicted. Training for this task typically experiences a skewed class imbalance as most pixels/patches usually correspond to a non-object class (i.e., no cancer). This is an issue as these non-object samples are easy to discriminate, preventing the learning process from prioritizing the minority of challenging training samples (i.e., isolated tumor cells and micro-metastasis). There are other machine learning tasks that are useful in the context of pathology image processing, such as content-based image.

Several submissions used transfer learning by fine-tuning pre-trained networks. In transfer learning, network weights are initialized when training for one task using the already established weights of a model pre-trained on a different task. This technique is commonly used when limited training data is available and allows for the abilities of a network trained on a larger data set to be leveraged. Thus, knowledge gathered by high-performing CNNs in general domains can be transferred to related domains, such as medical image analysis [19]. The ‘HMS-MGH’ and ‘CULab’ teams made use of transfer learning and were amongst the 3 teams that gave the highest performance submissions for both tumor localization and whole-slide classification. The CNNs used in systems ‘HMS-MGH III’, ‘HMS-MGH II’, and ‘CULabIII’ were ResNet-101, GoogLeNet-22 and VGG-Net-16, respectively. Each was initialized by weights from pre-trained networks and fine-tuned with the Camelyon-16 challenge data. ResNet-101 was pre-trained on the ‘MS-COCO’ data set and the other two models were pre-trained on the large scale 1000-class ‘ImageNet’ data set [20].

For the breakhis challenge, transfer learning is arguably beneficial as the associated data set contains just 270 labelled WSIs. With the use of patch sampling and data augmentation, the number of training samples can be extended to the order of hundreds of thousands; however, this is significantly smaller than the millions of training samples provided by the ‘MS-COCO’ and ‘ImageNet’ data sets. Despite this, Liu et al. suggest that network pre-training does not significantly improve model performance; there may be too large a domain difference between pathology images and natural scenes, as given by ‘ImageNet’ and ‘MS-COCO’, leading to limited knowledge transferability. They concede that this conclusion may arise from their use of extensive patch sampling and data augmentation, resulting in accurate models without pre-training. Regardless, network pre-training is observed to also improve model convergence speed.

Whilst unsupervised learning may allow for the existing wealth of unlabeled medical data to be leveraged, this project exclusively explores supervised learning. The aim of this project is to improve the clinical viability of existing state-of-the-art methods for breast cancer detection. Supervised approaches have been greatly explored in this field, and the existence of the Camelyon challenges permit meaningful comparisons to these approaches, which is not the case with unsupervised learning research. Additionally, two other nuanced machine learning algorithm types are semi-supervised learning [21] and

Jilin Daxue Xuebao (Gongxueban)/Journal of Jilin University (Engineering and Technology Edition)
ISSN：1671-5497
E-Publication: Online Open Access
Vol: 42 Issue: 03-2023
DOI 10.17605/OSF.IO/WNQ34

reinforcement learning [22]. Whilst these are growing research areas, most machine learning algorithms for automated breast cancer diagnosis are supervised.

Maksoud et al. presented a method for the selective use of high-resolution processing based on prediction confidence at low resolutions. Their system involves the use of a decision protocol to determine whether a low-resolution versus high-resolution network should be utilized. Their system was applied to 'liver-kidney-stomach' WSIs, where they were able to improve multi-class classification accuracy, whilst reducing inference time by a factor of 7.74 (when compared to other multi-scale approaches) [23]. This approach is said to build on similar prior work carried out by Dong et al. (2018), where breast cancer segmentation is carried out in WSIs using low- or high-resolution images, as determined by a trained policy network (via reinforcement learning) which decides whether zooming in on regions of interest is required [24]. A very different multi-scale approach is presented by Hering and Kybic (2020) to detect cancerous tissue in histological images (a subset of the Camelyon-16 data set). In their approach, several small regions of interest, which they call 'glimpses', are processed as opposed to the whole high-resolution WSI. The glimpses form a tree structure; glimpses at a low resolution determine the location of several higher resolution glimpses, continuing hierarchically until the highest resolution is reached. At the highest resolution, glimpses are classified and a whole-slide classification score is calculated (the maximum prediction score assigned to the highest resolution glimpses). They reported a mean AUC score between 0.92 and 0.95 (depending on their model parameters), which is comparable to the best AUC score (0.96) of the top performing Camelyon-16 team [13]. Their model inference time was between 1-1.5 seconds. This demonstrated that it is possible to perform high confidence classification having processed only a small proportion of the high-resolution image, leading to an important speedup with only a small performance deterioration [25].

In terms of single-resolution models using low-resolution images, the following recent approaches are notable: Patil et al. presented a CNN-based architecture for segmenting invasive breast cancer. The approach uses very low-resolution WSIs (320 x 320 pixels). The model is said to have achieved high accuracy when the cancerous regions took up a large proportion of the very low-resolution WSI but performed significantly worse for smaller cancerous regions [26]. This indicates that for this project, a developed low-resolution model may perform well on macro-metastases, which can be reasonably large in proportion to overall tissue but give an unsatisfactory performance at localizing micro-metastases. Zormpas-Petridis et al. presented a computationally efficient framework ('Super Histopath') designed to map global context features (by classifying and segmenting such features), reflecting the rich tumour morphological heterogeneity in WSIs (e.g., tumour tissue, stroma, necrosis, lymphocytes clusters, fat, hemorrhage and normal tissue). The approach involves the segmentation of low-resolution WSIs (at 5x magnification) into super-pixels, followed by classification of the super-pixels using a CNN ('Xception' and a custom CNN). It was shown that 'Super Histopath' is efficient for training and inference (~5 minutes for classifying a WSI, and as low as ~30 minutes for network training). For breast cancer WSIs, 'Super Histopath' classified sample regions into 6 predefined tissue categories of interest (tumour, necrosis, stroma, cluster of lymphocytes, fat, and lumen/empty space) with an overall accuracy of 93.1%, an average precision of

Jilin Daxue Xuebao (Gongxueban)/Journal of Jilin University (Engineering and Technology Edition)
ISSN：1671-5497
E-Publication: Online Open Access
Vol: 42 Issue: 03-2023
DOI 10.17605/OSF.IO/WNQ34

93.9%, and an average recall of 93.6% using ‘Xception’ (and 91.7%, 92.5%, 91.8% respectively using the custom CNN) over 10,349 super-pixels in an independent test set of five images [27].

Finally, Shahidi presented a novel super-resolution approach using a generative adversarial network to generate super-resolution images from low-resolution WSIs. Since the hardware and storage requirements of WSIs are great, this paper is motivated by the idea of being able to store WSIs at low resolution with the intention that super-resolution techniques can be applied to achieve classification performance on the super-resolution images comparable to performance using the original high-resolution versions. Despite this, the main factor of relevance from this work concerns the performance comparison of controlled models (ResNeXt-101) using low- (64 x 64-pixel patches) and high-resolution (256 x 256-pixel patches) images for tumor classification. The high-resolution images gave better performance (99.49% accuracy score), but not dramatically so compared to low-resolution images (95.82% accuracy score) [28].

In summary, single-resolution models using low-resolution images have seen some success for medical image analysis tasks. However, this does not indicate that the low-resolution model developed in this project will also give high confidence predictions; the differences in medical tasks being performed is a key factor. For example, a low-resolution model will be more capable at segmenting large tissue sub-types (especially when there is significant heterogeneity), than segmenting smaller homogeneous lesions (as is the case with the breakhis data sets). Otherwise, research is focused on multi-scale approaches that use low-resolution images by default but can resort to high-resolution processing when required. Since such approaches are designed to reduce inference time (on average) whilst maintaining high network capability, one may question the need for strictly low-resolution image models. However, it may be the case that strictly low-resolution models are sufficient for certain medical tasks, alleviating the hardware and storage requirements associated with maintaining high-resolution WSIs. Even when low-resolution model performance is inferior to multi-scale approaches, the low-resolution model may be exceptional for a certain class, warranting use. For example, a low-resolution model that exceptionally classifies benign tissue can filter the majority of negative cases, allowing pathologists to focus workload on challenging cases requiring attention.

3. METHODOLOGY

3.1 Deep Learning Framework

Due to the considerable memory requirements of the data sets employed and the complexity of the deep CNN models developed, a graphics processing unit (GPU) has been used to provide increased computational power. A ‘NVidia GeForce GTX 1060 (6GB)’ GPU was provided by Kaggle.com To take advantage of the computational capability provided by the GPU, a deep learning framework possessing CUDA support (for GPU acceleration) with CNN-based implementations has been selected: PyTorch (Paszke et al., 2019). PyTorch was chosen over similar alternatives, such as the more popular Tensor Flow (with Keras) framework, due to familiarity with PyTorch by the parties

Jilin Daxue Xuebao (Gongxueban)/Journal of Jilin University (Engineering and Technology Edition)
ISSN：1671-5497
E-Publication: Online Open Access
Vol: 42 Issue: 03-2023
DOI 10.17605/OSF.IO/WNQ34

involved in this project. Supplementary packages have been added to this framework, such as TorchVision/SKImage for image processing, Ray Tune for automated hyper-parameter optimization, and ASAP/Open Slide (which are provided by and recommended for the Kaggle challenges) for manipulating the high-resolution WSIs.

3.2 User Interface

A command-line interface (CLI) has been selected as sufficient, allowing for configurable execution via program arguments and flags. A full user manual for execution of the developed models (and supplementary tools) is included in section 8.4. Where model visualizations are beneficial, the popular Tensor Board package has been used for interpretation using a graphical user interface (GUI); example image outputs resulting from tissue detection and data augmentation are displayed, and model training is graphed (i.e., training/validation loss change per epoch), etc.

3.3 Whole-Slide Classification Design

The deep learning pipeline for whole-slide classification is characterized as simply reducing the high-resolution BreakHis data set images to a sufficiently small size such that they can be fed as input into a pre-trained CNN for binary classification (slides are cancerous or normal). However, additional techniques have also been employed to boost the general performance of this simple approach. The pipeline consists of four phases: pre-processing, model training, hyper-parameter optimization, and result reporting (as illustrated in Figure 1).

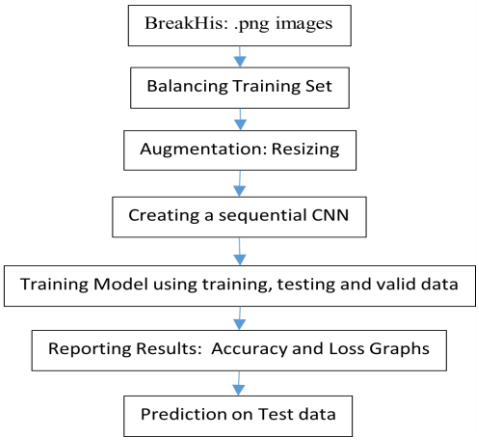

Figure 1: Block Diagram for Whole Slide Classification

3.4 Data Set

This section describes the data set used and explains any manipulations of this data set to assist model training and evaluation.

3.4.1 Data Set Decision:

There are 9,109 microscopic photos of breast tumour tissue from 82 individuals that were gathered for the Breast Cancer Histopathological Image Classification (BreakHis) using various magnification factors (40X, 100X, 200X, and 400X). It now has 2,480 benign and

Jilin Daxue Xuebao (Gongxueban)/Journal of Jilin University (Engineering and Technology Edition)
ISSN：1671-5497
E-Publication: Online Open Access
Vol: 42 Issue: 03-2023
DOI 10.17605/OSF.IO/WNQ34

5,429 cancerous samples (700X460 pixels, 3-channel RGB, 8-bit depth in each channel, PNG format). In cooperation with the P&D Laboratory - Pathological Anatomy and Cytopathology, Parana, Brazil (http://www.prevencaoediagnose.com.br), this database was created. This database enables future benchmarking and assessment; therefore, we think researchers will find it beneficial. The collection the two primary categories of BreakHis are benign tumors and malignant cancers. A lesion is said to as histologically benign if it does not meet any criteria for malignancy, such as significant cellular atypia, mitosis, breakdown of basement membranes, metastasis, etc. Normal benign tumors are slow-growing, confined growths that are considered "innocent." Cancer is referred regarded as a malignant tumour because the lesion has the ability to spread to distant areas (metastasize) and infect other structures, causing damage and eventual death.

The samples in the dataset in the current edition were obtained using the SOB procedure, commonly known as the partial mastectomy or excisional biopsy. Compared to other needle biopsy techniques, this type of operation extracts a bigger sample of tissue, and it is performed in a hospital under general anesthesia. Table 1 shows the distribution of images in BreakHis 1.0.:

Table 1: BreakHis structure [29]

Magnification	Benign	Malignant	Total
40X	625	1,370	1,995
100X	644	1,437	2,081
200X	623	1,390	2,013
400X	588	1,232	1,820
Total of Images	2,480	5,429	7,909

Based on how the tumoral cells appear under a microscope, benign and malignant breast tumors can be divided into many categories. Different breast tumour types and subtypes may have varying prognoses and therapeutic consequences. Adenosis (A), fibroadenoma (F), phyllodestumour (PT), and tubular adenona (TA) are the four histologically distinct types of benign breast tumors currently present in the dataset. Carcinoma (DC), lobular carcinoma (LC), mucinous carcinoma (MC), and papillary carcinoma are the four malignant tumors (breast cancer) currently present (PC). Each picture filename contains details about the image itself, including the biopsy method, the type of tumour, the patients identify, and the magnification level. For instance, SOB B TA-14-4659-40-001.png is the image 1 of a benign tumour of type tubular adenoma, with a magnification factor of 40X, which was originally taken from the slide 14-4659 and gathered by process SOB.

Jilin Daxue Xuebao (Gongxueban)/Journal of Jilin University (Engineering and Technology Edition)
ISSN：1671-5497
E-Publication: Online Open Access
Vol: 42 Issue: 03-2023
DOI 10.17605/OSF.IO/WNQ34

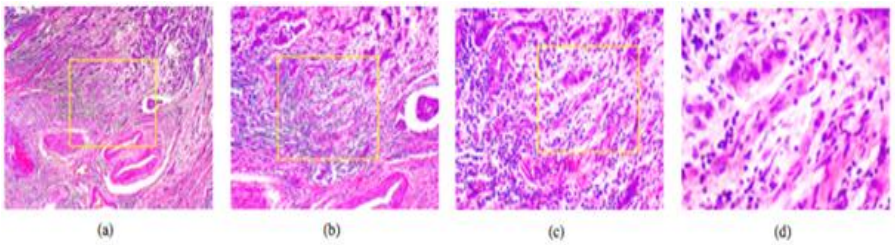

Figure 2: A slide of breast malignant tumor (stained with HE) seen in different magnification factors: (a) 40X, (b) 100X, (c) 200X, and (d) 400X [29]

3.4.2 Dataset Split

Dataset provided is separated in two main categories. So, we have divided it into three different categories training, testing and validation to feed it to convolutional neural network. Dataset was splinted into three sets as 6406, 712, 791 for training, validation and testing respectively. The model performs binary classification, so inspection of the output class distribution was crucial in determining whether re-balancing was required to prevent model bias towards one of the output classes (see Figure 3.3). The BreakHis training data has a positive (i.e., cancer) class proportion of ~ 38%, which reflects the real-world statistic that 60-70% of extracted sentinel lymph nodesdo not contain metastases [30].Whilst the observed output class imbalance is not severe, re-balancing prevents any minor class bias.

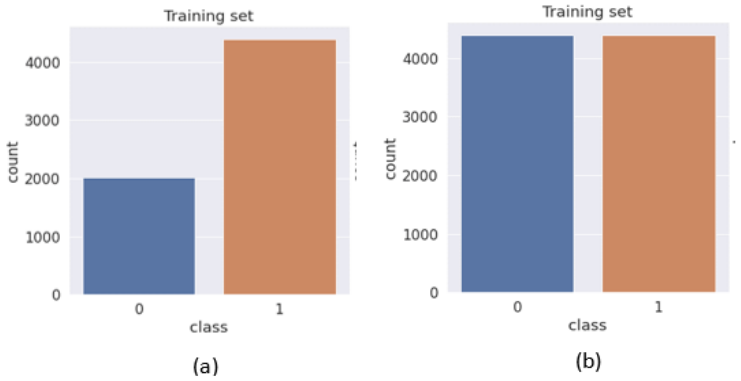

Figure 3: Spliting Dataset

Various solutions to re-balance the data were considered. Under-sampling would involve dropping normal slides to equal the number of cancer slides, but this would diminish the limited amount of majority class data and, therefore, possibly discard useful features. Over-sampling the minority class through the use of, say, the synthetic minority over-sampling technique (SMOTE) [20] would balance the output classes and increase the amount of useful information available to the model, but this is more computationally expensive compared to the simpler technique used: class weights. Class weighting applies greater importance to the under-represented class when computing the loss function and does not require additional manipulation of the training data. The use of SMOTE for image data could be investigated in future work given its capability to

Jilin Daxue Xuebao (Gongxueban)/Journal of Jilin University (Engineering and Technology Edition)
ISSN：1671-5497
E-Publication: Online Open Access
Vol: 42 Issue: 03-2023
DOI 10.17605/OSF.IO/WNQ34

meaningfully increase the size of the training data set, which is currently limited in BreakHis 1.0.

3.4.3 Label Encoding

The labels for the output classes are provided in categorical string format, but they were converted to numerical format, which is required for model training and inference. As the model performs binary classification, a simple binary encoding of the target classes has been used (see Table 2).

Table 2: Table showing binary encoding of the output classes.

Category Label	Binary Encoding
'Benign' (or 'None' or 'Negative')	0
'Malignant' (or 'ITC ' or 'Micro' or 'Macro')	1

3.5 Pre-Processing

Any data augmentation used is applied to the training images; however, data preparation is performed on all images (i.e., train, validate, and test) as a pre-processing step immediately before feeding the images as model input. Data preparation consists of image resizing and normalization. Image resizing involves converting the low-resolution .PNG images into target low-resolution dimensions desired for investigation. As an initial choice, image sizes of 128 x 128 pixels were used. This is the smallest input size permitted by the chosen CNN architecture. Based on the assumption that the model will likely perform worse as image resolution is decreased (discussed in the context survey - see chapter 2), investigating the input dimensions of 128 x 128 pixels will establish a lower-bound for model performance. The BreakHis submissions provide an upper-bound for model performance using high-resolution images. From this, the input resolution is explored further within these bounds with the intent to find an optimal resolution that maximizes prediction confidence whilst minimizing resource requirements.

The further image resolutions investigated are: 512 x 512, 1024 x 1024, and 2048 x 2048 pixels. Investigating greater input resolutions (4096 x 4096 pixels, etc.) is also justified as these resolutions are still low-resolution being thousands of times smaller than the original data set images. However, such resolutions are increasingly infeasible for investigation given the memory constraints they impose, ultimately requiring significant training time (larger image resolutions push the limit on the fact that these images are given in their entirety as input to a CNN for classification). To handle increasing input images resolutions (above the original 128 x 128 pixels), whilst maintaining the same batch size (at 16), an accumulated gradient approach was implemented for use with larger image resolutions that would otherwise create out-of-memory issues. The accumulated gradient approach essentially sets the batch size as 1 so that individual images are loaded into memory. However, the network is only updated once the required batch size number of images (i.e., 16) have had their losses computed. This is effectively the same as just using the required batch size, but memory management is utilized for practical purposes.

A noted issue of the image resizing is that images are morphed to a square (1:1) aspect ratio. As a result, the model versions seek to identify general features to classify cancer

Jilin Daxue Xuebao (Gongxueban)/Journal of Jilin University (Engineering and Technology Edition)
ISSN：1671-5497
E-Publication: Online Open Access
Vol: 42 Issue: 03-2023
DOI 10.17605/OSF.IO/WNQ34

in ‘squashed’ WSIs. The tissue morphing negatively affects classification ability as any information on the shape of cell and multi-cellular structures is damaged. The Kaggle submissions were able to use square inputs without issue as they used random cropping of high-resolution WSIs to create training patches; cropping an image does not distort the image content. In this project, however, the WSIs themselves are used as input and do not all have uniform dimensions (required by the CNN architecture), so resizing must be applied. Finally, the training images are normalized, which is a common pre-processing step to improve training by increasing model numerical stability and/or speeding up the training process. The model was initially trained without normalization, then with the normalization values recommended for the PyTorch CNN sequential model, and finally with normalization values calculated for the BreakHis low-resolution training WSIs.

3.6 Model Training

This section outlines the design pertaining to model training carried out using the pre-processed WSIs (see Figure 4).

3.7 Deep CNN Architecture

The majority of successful submissions to the BreakHis challenges used a select few deep learning architectures, primarily GoogLeNet, AlexNet, or VGG-Net. Whilst each of these architectures are viable choices for this project’s low-resolution models, ultimately, a GoogLeNet based architecture was selected as this was used by the top performing ‘HMS-MIT’ team for the whole-slide classification task. Specifically, the Inception v3 architecture (a newer version of GoogLeNet, also known as Inception v1) was selected as this provides several iterations of improvement upon the original GoogLeNet design.

The proposed CNN architecture could have been substituted for the other viable architectures (e.g., AlexNet and VGG-Net) to determine concretely which architecture is best suited for breast cancer detection using low-resolution images. Furthermore, the predictions of these different models could have been aggregated to form an ensemble, which was a technique observed with many BreakHis submissions, to determine if general performance could be even further improved. Assuming the ensemble models could infer via parallel processing, and that there is no significant disparity between their inference times, the use of an ensemble could improve prediction performance with little expense to the overall average inference time.

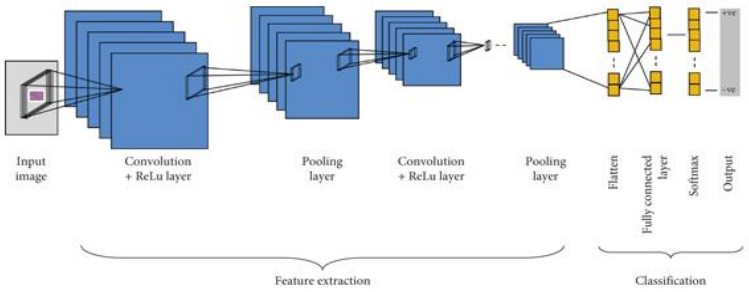

Figure 4: Proposed CNN Architecture

Jilin Daxue Xuebao (Gongxueban)/Journal of Jilin University (Engineering and Technology Edition)
ISSN：1671-5497
E-Publication: Online Open Access
Vol: 42 Issue: 03-2023
DOI 10.17605/OSF.IO/WNQ34

3.8 Loss Function

The selected loss function is binary cross entropy loss (also known as log loss), which is a standard machine learning choice for binary classification tasks [10]. Binary cross entropy compares each predicted output probability to its corresponding actual output. An overall score is calculated which penalizes the predicted probabilities based on distance from their expected output. Usefully, loss increases exponentially the more incorrect (greater the distance) a predicted probability is from the expected output (i.e., large penalties deter the model from predicting low probabilities for positive class samples).

3.9 Optimizer

Due to the complexity involved with the deep nature of the CNN model, it is key to minimize the number of hyper-parameters to tune. Adaptive learning rate optimization algorithms provide good out-of-the-box performance via fast convergence and little parameter fine-tuning when compared with traditional optimization algorithms, such as stochastic gradient decent (SGD). The most generally used adaptive optimizer is adaptive moment estimation (Adam), which combines momentum (for larger steps in the direction of the steepest gradient) and root mean square propagation (for higher acceleration on steep slopes). Adam was selected as a suitable optimizer for these qualities, though many different optimizers and many variations of Adam itself exist. An improvement would be to perform an empirical investigation as to which optimizer yields the best performance for the BreakHis data set. This was not prioritized due to the complex interplay of model variables, where a change to one variable may alter the best choice for all other variables, so great effort would need to be expended for what would be tantamount to a limited gain in terms of the project objectives.

3.10 Early Stopping

As discussed, the original training data was separated into training and validation partitions with an 80%/20% split respectively. At the end of each training epoch, model predictions are performed on the validation set to obtain an epoch validation loss. Training is halted if this validation loss has not decreased significantly within some number of epochs to prevent over-fitting on the training data. The number of epochs permitted without improvement was configured as 10% of the maximum number of epochs for training. This proportion balances the need to prevent over-fitting, whilst permitting sufficient patience as to not prematurely stop training due to local minima.

An improvement to this design would be to use K-fold cross validation, which allows for training using all of the available training data (especially useful given the limited size of the training data set), prevention of validation set over-fitting, and more accurate reporting of model performance on unseen data. However, K-fold cross validation divides the training data into K subsets and effectively trains K different models (each training on different K - 1 subsets and evaluating on the final Kth subset). Due to project time constraints, the required time to train a model (in the order of hours and emphasized by the presence of several model versions requiring hyper-parameter optimization with a broad search space), and an unfamiliarity with its implementation in PyTorch, the use of K-fold cross validation was not prioritized and a simple validation set was opted for.

Jilin Daxue Xuebao (Gongxueban)/Journal of Jilin University (Engineering and Technology Edition)
ISSN：1671-5497
E-Publication: Online Open Access
Vol: 42 Issue: 03-2023
DOI 10.17605/OSF.IO/WNQ34

4. RESULTS AND DISCUSSION

Figure shows training and validation accuracies with respect to each epoch with learning rate of 0.001. Model outperformed on this challenge dataset of histopathology images. We have used 80% of images having magnification level of 40x, 100x, 200x, 400x for training. Table shows division of dataset.

Table 3: Train Test Split

Class	Training	Validation	Test
Benign	4398	211	261
Malignant	4398	501	530

CNN model was evaluated using binary cross entropy and results are shown in following figure.

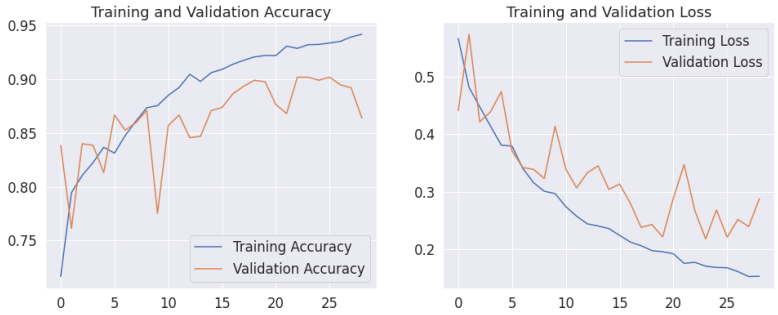

Figure 5: Training and validation performance

The over-curving result concerning this project is the grown deep education passage for twofold malignancy categorization is efficiently ability-less at the examined depressed recommendation judgments, even when supplementary methods were achieved to advance comprehensive efficiency. This project's deep education passage can have raised skillfulness at best recommendation determinations than those examined, probably disclosing few optimum judgment that captures adequate prophecy depiction and average deduction period. However, this appears improbable likely that skilled performs expected a basic adjustment middle from two points two together requested attributes, needing an inadequate resolution to plan out either model act or deduction speed to delimit the recommendation judgment to use. This is not the case accompanying the considered multi-judgment approaches. Currently, this project's models contract an illness the 'refuse-in, refuse-out' characteristic accredit the flight data recorder character of deep knowledge models. The reduced-judgment recommendation figures, are considerably clouded at the natural level, making the labeling of inevitable physiognomy for malignancy discovery (container bulk, shape unevenness, discoloring, etc.) uncertain even by prepared pathologists. It can again endure that the passage is innately container-kiss by any means recommendation determinations for one restricted amount of preparation samples feasible. Simply, skilled is insufficient branded preparation samples for the model to determine by means of what to foresee metastases inside comparable performing fabric, particularly likely that skilled are diversified types of malignancy that

Jilin Daxue Xuebao (Gongxueban)/Journal of Jilin University (Engineering and Technology Edition)
ISSN：1671-5497
E-Publication: Online Open Access
Vol: 42 Issue: 03-2023
DOI 10.17605/OSF.IO/WNQ34

the model is trying to combine for categorization (that is, data processing machine-metastases, big-metastases, ITCs). This is an basic issue of utilizing WSIs as inputs in their wholeness, because the amount of the preparation basic document file enhances connected to the number of WSIs that can fairly be thoroughly commented by prepared healing work force. In summary, the grown deep knowledge passage has happened proved expected lacking even when the recommendation determination has happened raised to 512 x 512 and 1024 x 1024 pixels. A slight noticed increase inaccuracy score (as the recommendation judgment has existed raised) signifies that the models are flattering less helpless at divorcing the outputs, suggesting that few up until now different minimum determination is necessary for class break-up and better than chance forecasts. However, the benefit of further search to find aforementioned a recommendation determination is doubtful likely the growing in-practicability of preparation CNNs utilizing these best determination representations completely as recommendation. For example, attempts to question 2048 x 2048-pel inputs were ineffectual as the model acted not reach union following in position or time various days of preparation. Although, the practicability of model preparation depends on applicable supplies, assigned preparation period, and seen benefit of the developing model, so no claims maybe fashioned that future work fact-finding best recommendation judgments would not be advantageous. Furthermore, prepared model has realized 94.88% of preparation and 91.04% of experiment veracity at allure best do an impression of preparation by 49 epochs before this time.

5. CONCLUSION

The basic restraint concerning this article is that the design and exercise of the reduced-judgment tumor discovery models are principally in theory argued, as opposed to tentatively examine. The growth passage has happened legitimized utilizing best practices noticed accompanying the BreakHis challenge compliances and appropriate tumor discovery models in the inexact field of healing representation study. It stands that future work bears complete activity practical inspections of center passage facets, admitting for the efficiency of the methods secondhand (that is, plainly lowering the extreme-determination concepts expected amply limited enough that they may bea recommendation to a CNN) expected completely earned. Whilst diversified methods have happened surveyed to raise the open ocean education passage, the methods are continual because a twofold tumor categorization CNN is used to judgment weakened study of plants concepts. For example, the methods of absolutely lowering the WSIs to a littleness and augmenting all figures as recommendations to a CNN commit to bringing about a productive classifier of abundant large-metastases that may be used to fast categorize cases concerning this type of tumor. Finally, this article proposed to help the dispassionate being of the BreakHis challenge compliances. More realistically, this article proposed to forge a model that manages first be used to percolate out surely classifiable cases before utilizing a few existent BreakHis models for the surplus troublesome cases. In specific a synopsis, the haste of utilizing a depressed-judgment model to percolate most distant cases commit substantiate the more interminable conclusion periods provoked apiece extreme-operating BreakHis compliances. However, neither of this

Jilin Daxue Xuebao (Gongxueban)/Journal of Jilin University (Engineering and Technology Edition)
ISSN：1671-5497
E-Publication: Online Open Access
Vol: 42 Issue: 03-2023
DOI 10.17605/OSF.IO/WNQ34

synopsis were earned, stressing the end that future work is necessary for fact-finding multi-determination approaches.

References

1. A. Madabhushi and G. Lee, “Image analysis and machine learning in digital pathology: Challenges and opportunities,” Med. Image Anal., vol. 33, pp. 170–175, 2016.
2. ARSLAN AKRAM et al, “A Robust And Scale Invariant Method For Image Forgery Classification Using Edge Weighted Local Texture Features,” JJU, vol. 41, no. 12–2022, pp. 330–344, Dec. 2022, doi: 10.17605/OSF.IO/MVWDU.
3. A. Akram, S. Ramzan, A. Rasool, A. Jaffar, U. Furqan, and W. Javed, “Image splicing detection using discriminative robust local binary pattern and support vector machine,” World J. Eng., vol. 19, no. 4, pp. 459–466, Jun. 2022, doi: 10.1108/WJE-09-2020-0456.
4. T. Mustafa, G. Ali, A. Akram, A. Tariq, M. U. Tariq, and M. S. Ali, “Cross-Cultural Facial Expression Recogniton Using Gradient Features And Support Vector Machine,” JJU, vol. 42, no. 1, pp. 386–406, Jan. 2023, doi: 10.17605/OSF.IO/XWZTK.
5. Sobia Yaqoob et al, “A Novel Method For Image Based Breast Cancer Classification,” JJU, vol. 41, no. 12–2022, pp. 470–484, Dec. 2022, doi: 10.17605/OSF.IO/JZFRM.
6. Muhammad Usman Tariq et al, “Real Time Age And Gender Classification Using Vgg19,” JJU, vol. 41, no. 12–2022, pp. 641–655, Dec. 2022, doi: 10.17605/OSF.IO/BKJWH.
7. Muhammad Salman All et al., “Chest X-Ray Based Pneumonia Classification Using Vgg-19,” JJU, vol. 42, no. 01–2023, pp. 118–136, Jan. 2023, doi: 10.17605/OSF.IO/M2FPD.
8. “Prognostic Factors and Survival Outcomes among Patients with Breast Cancer and Brain Metastases at Diagnosis: A National Cancer Database Analysis - Abstract - Oncology 2021, Vol. 99, No. 5 - Karger Publishers.” https://www.karger.com/Article/Abstract/512212 (accessed Feb. 20, 2023).
9. H. W. Rogers, M. A. Weinstock, S. R. Feldman, and B. M. Coldiron, “Incidence estimate of nonmelanoma skin cancer (keratinocyte carcinomas) in the US population, 2012,” JAMA Dermatol., vol. 151, no. 10, pp. 1081–1086, 2015.
10. G. Litjens et al., “1399 H&E-stained sentinel lymph node sections of breast cancer patients: the CAMELYON dataset,” GigaScience, vol. 7, no. 6, p. giy065, 2018.
11. Y. Yue et al., “Highly self-healable 3D microsupercapacitor with MXene–graphene composite aerogel,” Acs Nano, vol. 12, no. 5, pp. 4224–4232, 2018.
12. P. Bandi et al., “From detection of individual metastases to classification of lymph node status at the patient level: the camelyon17 challenge,” IEEE Trans. Med. Imaging, vol. 38, no. 2, pp. 550–560, 2018.
13. B. E. Bejnordi et al., “Diagnostic assessment of deep learning algorithms for detection of lymph node metastases in women with breast cancer,” Jama, vol. 318, no. 22, pp. 2199–2210, 2017.
14. N. Albert and D. Basavesha, “An Automatic Helmet Detection System using Convolution Neural Network,” Int. J. Adv. Sci. Innov., vol. 4, no. 3, 2022.
15. [V. Bevilacqua, A. Brunetti, M. Triggiani, D. Magaletti, M. Telegrafo, and M. Moschetta, “An optimized feed-forward artificial neural network topology to support radiologists in breast lesions classification,” in Proceedings of the 2016 on Genetic and Evolutionary Computation Conference Companion, 2016, pp. 1385–1392.
16. J. Griffin and D. Treanor, “Digital pathology in clinical use: where are we now and what is holding us back?,” Histopathology, vol. 70, no. 1, pp. 134–145, 2017.

Jilin Daxue Xuebao (Gongxueban)/Journal of Jilin University (Engineering and Technology Edition)
ISSN：1671-5497
E-Publication: Online Open Access
Vol: 42 Issue: 03-2023
DOI 10.17605/OSF.IO/WNQ34

17. T. Mendonça, P. M. Ferreira, J. S. Marques, A. R. Marcal, and J. Rozeira, “PH 2-A dermoscopic image database for research and benchmarking,” in 2013 35th annual international conference of the IEEE engineering in medicine and biology society (EMBC), 2013, pp. 5437–5440.
18. S. Russell and P. Norvig, “Artificial intelligence: a modern approach, Hoboken.” USA: Pearson, 2020.
19. R. Mormont, P. Geurts, and R. Marée, “Comparison of deep transfer learning strategies for digital pathology,” in Proceedings of the IEEE conference on computer vision and pattern recognition workshops, 2018, pp. 2262–2271.
20. O. Russakovsky et al., “Imagenet large scale visual recognition challenge,” Int. J. Comput. Vis., vol. 115, no. 3, pp. 211–252, 2015.
21. D. Suganya, K. Thirunadana Sikamani, and J. Sasikala, “Copy-move forgery detection of medical images using golden ball optimization,” Int. J. Comput. Appl., pp. 1–9, 2021.
22. R. S. Sutton and A. G. Barto, Reinforcement learning: An introduction. MIT press, 2018.
23. A. Alqudah and A. M. Alqudah, “Sliding window based support vector machine system for classification of breast cancer using histopathological microscopic images,” IETE J. Res., vol. 68, no. 1, pp. 59–67, 2022.
24. N. Dong, M. Kampffmeyer, X. Liang, Z. Wang, W. Dai, and E. Xing, “Reinforced auto-zoom net: towards accurate and fast breast cancer segmentation in whole-slide images,” in Deep Learning in Medical Image Analysis and Multimodal Learning for Clinical Decision Support, Springer, 2018, pp. 317–325.
25. J. Hering and J. Kybic, “Multiple instance learning via deep hierarchical exploration for histology image classification,” in 2020 IEEE 17th International Symposium on Biomedical Imaging (ISBI), 2020, pp. 235–238.
26. S. M. Patil, L. Tong, and M. D. Wang, “Generating region of interests for invasive breast cancer in histopathological whole-slide-image,” in 2020 IEEE 44th Annual Computers, Software, and Applications Conference (COMPSAC), 2020, pp. 723–728.
27. K. Zormpas-Petridis, R. Noguera, D. K. Ivankovic, I. Roxanis, Y. Jamin, and Y. Yuan, “Superhistopath: a deep learning pipeline for mapping tumor heterogeneity on low-resolution whole-slide digital histopathology images,” Front. Oncol., vol. 10, p. 586292, 2021.
28. F. Shahidi, “Breast cancer histopathology image super-resolution using wide-attention gan with improved wasserstein gradient penalty and perceptual loss,” IEEE Access, vol. 9, pp. 32795–32809, 2021.
29. “Breast Cancer Histopathological Database (BreakHis) - Laboratório Visão Robótica e Imagem,” Jun. 20, 2017. https://web.inf.ufpr.br/vri/databases/breast-cancer-histopathological-database-breakhis/ (accessed Dec. 27, 2022).
30. J. Kim, H. Park, and J.-I. Park, “CNN-based image steg analysis using additional data embedding,” Multimed. Tools Appl., vol. 79, no. 1, pp. 1355–1372, 2020.